

Supporting Information

Reversible Switching of Slow Magnetic Relaxation in a Classic Lanthanide Metal-Organic Framework System

Qi Zhou, Fen Yang, Bingjing Xin, Guang Zeng, Xiaojing Zhou, Kang Liu, Dingxuan Ma, Guanghua Li*, Zhan Shi,* and Shouhua Feng

State Key Laboratory of Inorganic Synthesis & Preparative Chemistry,
College of Chemistry, Jilin University, Changchun 130012, P. R. China.
E-mail: zshi@mail.jlu.edu.cn; leegh@jlu.edu.cn

Synthesis

All reagents and solvents were commercially available and were used without further purification.

Dy(BTC)(H₂O)DMF (1) was synthesized using the procedures reported previously.¹ A mixture of Dy(NO₃)₃·6H₂O (45mg, 0.1mmol) and H₃BTC (0.02mg 0.1mmol) was dissolved in DMF (10mL), distilled water (2mL) and cyclohexanol (2mL). Then two drops of dibutylamine and three drops of HNO₃ (2 mol·L⁻¹) were added. The mixture was stirred in a 50-mL beaker for 2h at room temperature and placed in an oven at 85 °C for 16h. The colorless products were collected by filtration, washed with DMF and methanol, and dried at room temperature. Yield: ca. 53%. Elem anal. Calcd (%) for C₁₂H₁₂DyNO₈: C, 31.28; H, 2.63; N, 3.04. Found: C, 31.26; H, 2.62; N, 3.02. IR (KBr, cm⁻¹): 3385(m), 1616(s), 1573(m), 1538(m), 1442(s), 1380(s), 1106(w), 940(w), 771(m), 705(m), 665(w), 557(w), 460(w), 430(w).

Dy(BTC) (2) was obtained by heating **1** under vacuum at 240 °C for 12h. IR (KBr, cm⁻¹): 1617(s), 1579(m), 1529(m), 1442(s), 1383(s), 1107(w), 940(w), 774(m), 705(m), 656(w), 567(w), 466(w), 432(w).

The rehydrated phase **1a** was obtained by steeping **2** in the mixture of water and DMF (1:1) for 2h at room temperature. Elem anal. Calcd (%) for C₁₂H₁₂DyNO₈: C, 31.28; H, 2.63; N, 3.04. Found: C, 31.22; H, 2.60; N, 3.05. IR (KBr, cm⁻¹): 3389(m), 1615(s), 1570(s), 1540(m), 1435(s), 1375(s), 1119(w), 939(w), 774(m), 713(m), 660(w), 563(w), 458(w), 428(w).

TG-DTA curves reveal that the dehydration process was finished above 350 °C in the air (Fig. S7). When we decreased the reaction temperature or reaction time, such as heating compound **1** under vacuum at 200 °C for 12 h or 240 °C for 6 h, single crystal X-ray diffraction revealed that the terminal water molecules could not be removed completely. So in order to ensure the completeness of dehydration, we decided to heat compound **1** at 240 °C for 12 h. We also examined the changes in compound **2** upon exposure to H₂O vapor. We found that the single crystal samples were transformed into powder, and XRPD showed that the crystal structures had totally changed (Fig. S2). Therefore, we think DMF is necessary for the single-crystal-to-single-crystal transformation. The addition of DMF molecules may promote the rearrangement of metal ions and BTC molecules and stabilize the structures. This phenomenon has been reported in similar lanthanide-based MOFs.¹

Physical Measurements.

All magnetic data were obtained with a Quantum Design MPMS SQUID VSM magnetometer. The variable-temperature magnetic susceptibility was measured with an external magnetic field of 10000

Oe. Alternating current magnetic susceptibility measurements were performed in an oscillating ac field of 3.0 G. Samples were fixed in gelatin capsules and held in a brass sample holder. Pascal's constants were used to estimate the diamagnetic corrections, which were subtracted from the experimental susceptibilities to give the molar paramagnetic susceptibilities (χ_M). Elemental analyses of carbon, nitrogen and hydrogen were carried out on a Perkin-Elmer 240C elemental analyzer. IR spectra as KBr pellets were recorded with a Magna 750 FT-IR spectrophotometer using reflectance technique over the range of 4000-400 cm^{-1} . X-ray powder diffraction (XRPD) patterns were taken on a Rigaku D/max 2550 X-ray Powder Diffractometer. TG analysis was performed with a Perkin-Elmer TGA7 instrument at a ramp rate of 10°C/min in air.

X-ray Crystallography.

Single-crystal structure determination of **1**, **2**, and **1a** was carried out on a Rigaku RAXIS-RAPID diffractometer equipped with graphite-monochromated Mo- $K\alpha$ radiation ($\lambda = 0.71073 \text{ \AA}$) at 293 K. The intensity data sets were collected with the ω -scan technique and reduced by CrystalClear software. The structures were solved by direct methods and refined with the full-matrix leastsquares technique using the program SHELXTL.² The location of metal atom was easily determined, and O, N and C atoms were subsequently determined from the difference Fourier maps. Anisotropic thermal parameters were assigned to all non-hydrogen atoms. The disordered atoms were refined with constrained dimensions. The hydrogen atoms were set in calculated positions. All compounds were treated with SQUEEZE. The crystal data, data collection and refinement parameters for **1**, **2**, and **1a** are listed in Table S2. CCDC reference number for **2** is 936103.

Table S1. Distortion values calculated for the Dy^{III} ions geometry.

Compound	Coordination	S(D_{5h})	S(C_{3v})	S(C_{2v})
Compound 1	Heptacoordinate	3.795	8.95	5.88
Compound 2	Hexacoordinate Dy1	S(C_{5v}) 15.22	S(O_h) 10.04	S(D_{3h}) 5.64

S = symmetry

Table S2. Crystallographic data for **1**, **2**, and **1a**.

compound	1	2	1a
formula	C ₉ H ₅ DyO ₇	C ₉ H ₃ DyO ₆	C ₉ H ₅ DyO ₇
fw (g mol ⁻¹)	387.63	369.61	387.63
cryst syst	tetragonal	tetragonal	tetragonal
space grp	<i>P</i> 4 ₃ 22	<i>P</i> 4 ₃ 22	<i>P</i> 4 ₃ 22
<i>a</i> (Å)	10.3091(15)	10.3509(15)	10.3028(15)
<i>b</i> (Å)	10.3091(15)	10.3509(15)	10.3028(15)
<i>c</i> (Å)	14.498(3)	13.916(3)	14.507(3)
<i>V</i> (Å ³)	1540.9(4)	1490.9(4)	1539.9(4)
<i>Z</i>	4	4	4
<i>F</i> (000)	724	684	724
μ (mm ⁻¹)	4.863	5.017	4.866

$D_{calcd}(\text{g cm}^{-3})$	1.671	1.647	1.672
$T(\text{K})$	293	293	293
R_1^a	0.0239	0.0197	0.0409
wR_2^b	0.0882	0.0455	0.1295

$$^a R_1 = \frac{\sum ||F_o| - |F_c||}{\sum |F_o|}; \quad ^b wR_2 = \left\{ \frac{\sum [w(F_o^2 - F_c^2)^2]}{\sum [w(F_o^2)]^2} \right\}^{1/2};$$

$$w = 1/[\sigma^2 |F_o|^2 + (0.0511P)^2 + 19.56P], \text{ where } P = [|F_o|^2 + 2|F_c|^2]/3.$$

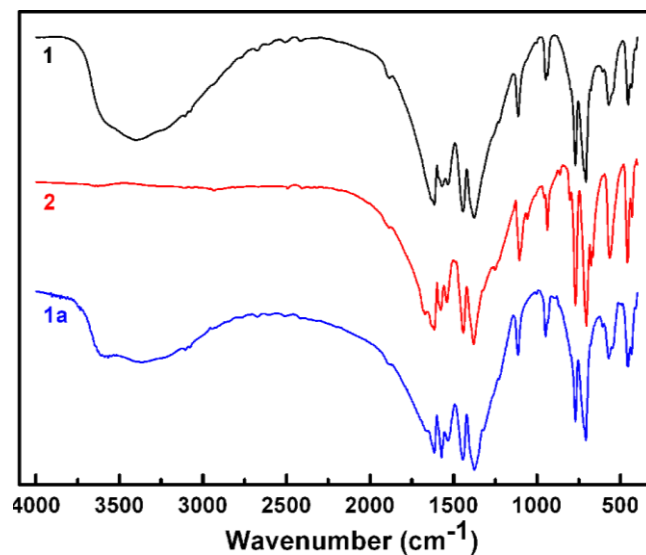


Fig. S1 IR spectra of 1, 2, and 1a.

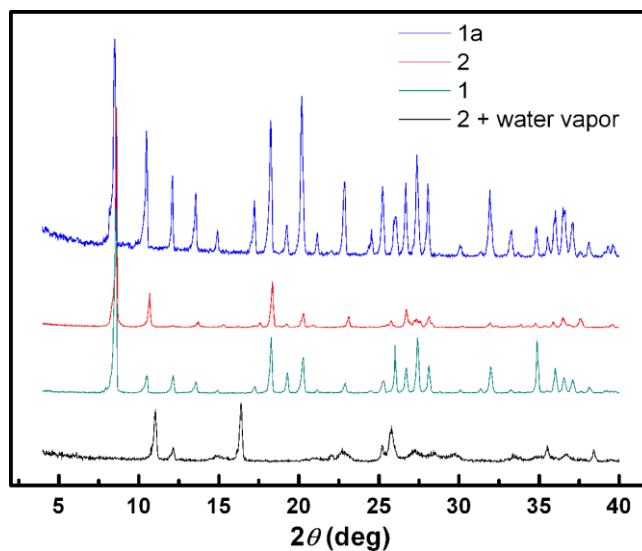


Fig. S2 XRPD pattern for 1, 2, and 1a.

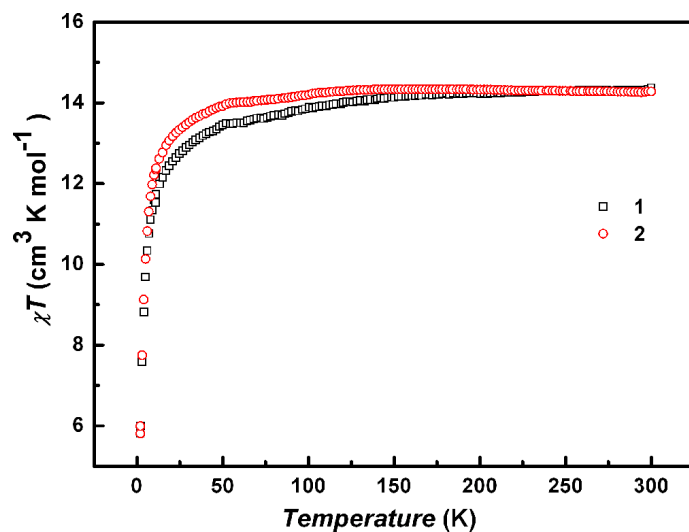


Fig. S3 Temperature dependence of the $\chi_M T$ product for **1** and **2** at 10000 Oe.

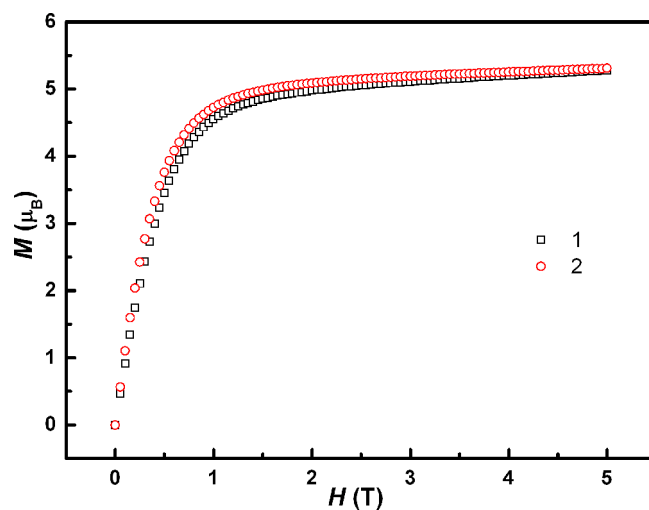


Fig. S4 Field dependence of the magnetization for **1** and **2** at 2K.

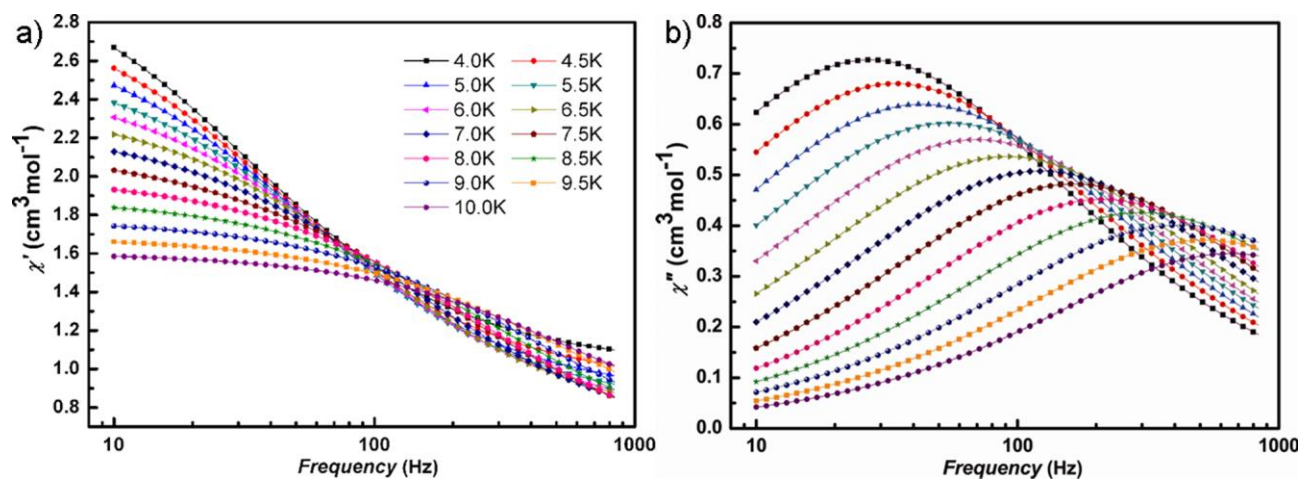


Fig. S5 Frequency dependence of in-phase (a) and out-of-phase (b) ac susceptibilities for **2** in 1000 Oe dc field.

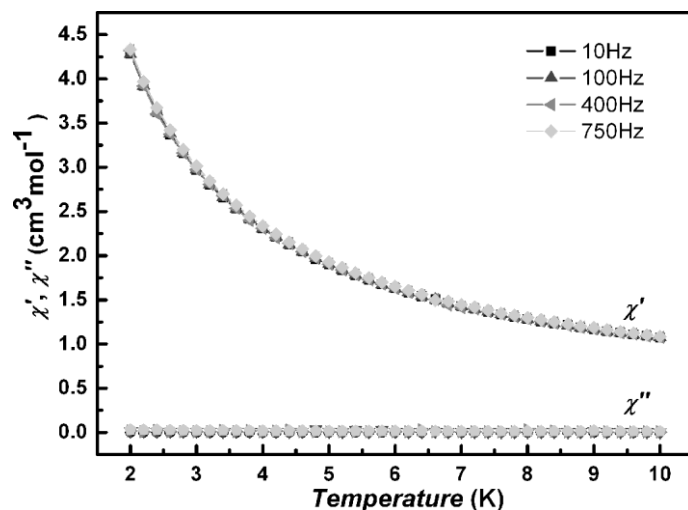


Fig. S6. Temperature dependence of the in-phase and out-of-phase ac susceptibility for **1a** under zero dc field.

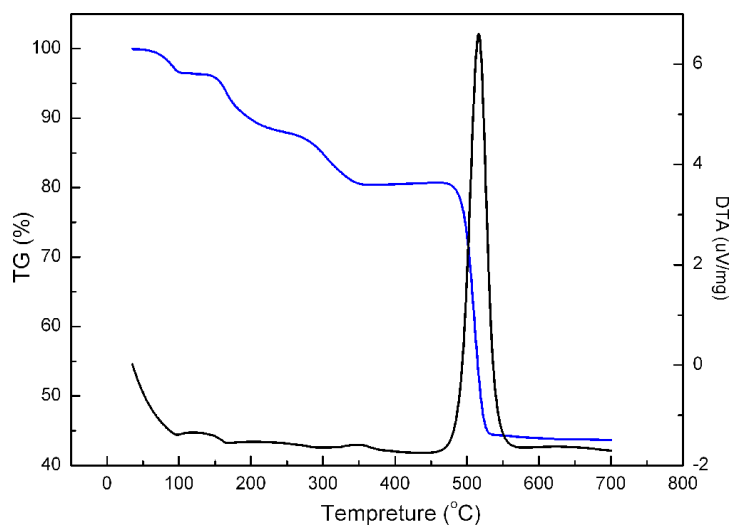


Fig. S7. TG-DTA curves for compound **1**

References

1. M. Gustafsson, A. Bartoszewicz, B. Martín-Matute, J. Sun, J. Grins, T. Zhao, Z. Li, G. Zhu, X. Zou, *Chem. Mater.*, 2010, **22**, 3316.
2. Sheldrick, G. M. SADABS, *Siemens Area Detector Absorption Correction*, University of Göttingen: Göttingen, Germany, 2005.